



A comparative study on the empirical modeling of photo-Fenton treatment process performance

M. Pérez-Moya^{a,*}, M. Graells^a, P. Buenestado^b, H.D. Mansilla^c

^a Departament d'Enginyeria Química, EUETIB, Universitat Politècnica de Catalunya, c/Comte d'Urgell, 187 Barcelona, Spain

^b Departament de Matemàtica Aplicada III, EUETIB, Universitat Politècnica de Catalunya, c/Comte d'Urgell, 187 Barcelona, Spain

^c Facultad de Ciencias Químicas, Universidad de Concepción, Concepción, Chile

ARTICLE INFO

Article history:

Received 19 February 2008

Received in revised form 3 April 2008

Accepted 5 April 2008

Available online 18 April 2008

Keywords:

Modeling

Experimental design

Photo-Fenton

4-Chlorophenol

ABSTRACT

This paper investigates the Fenton photo-assisted degradation of 4-chlorophenol (4-CP). The experimental work was planned according to the Design of Experiments (DOE) scheme, and degradation performance was measured in terms of TOC reduction at different reaction times. Appropriate reagent ratios have been obtained for effective 4-CP degradation.

The modeling of the process performance as a function of the reaction conditions was then studied by fitting different models to the degradation data. The models are compared and discussed according to the degree of correlation they provide. The widely used second order polynomial equation (including bilinear terms) is questioned and alternative models are proposed (potential model, Hoerl equation) for a better empirical representation of the performance of the degradation process.

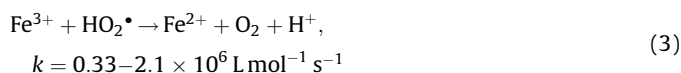
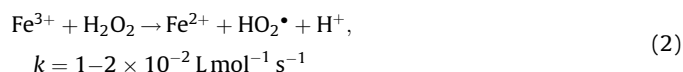
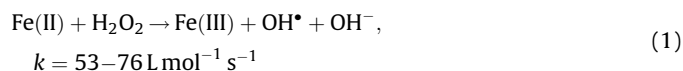
The disparate estimations given by the different models studied suggest that further research is required in model selection in order to obtain reliable characterization of Fenton, Fenton-like and photo-Fenton treatment performance.

© 2008 Elsevier B.V. All rights reserved.

1. Introduction

The simultaneity of Fenton, Fenton-like and photo-Fenton processes have revealed effective in the mineralization of 4-chlorophenol (4-CP). Particularly, the photochemically enhanced degradation process using Fenton reagent has been widely studied for coping with the problems this refractory contaminant [1–4] poses to wastewater treatment.

Although, the generally accepted Fenton mechanism has been known for longer than a century, Eq. (1) [5], the enhancement of process performance is still widely discussed in recent literature. Fe(III) can react with H₂O₂ in the so-called Fenton-like reaction, Eqs. (2) and (3), regenerating Fe(II) and thus supporting the Fenton process [6]:



The degradation rate of the organic pollutants by Fenton reaction could increase when an irradiation source is present. The positive effect of irradiation on the degradation rate is due to the photo-reduction of Fe(III) to Fe(II) ions, a step that produces new OH[•] radicals and regenerates Fe(II) ions that can further react with more H₂O₂ molecules. The photoreduction of Fe(III) follows Eq. (4) [7]



For detailed reaction paths and kinetic parameters, readers should refer to [6–11].

The photo-assisted Fenton degradation process is a multifactor system. For this reason the characterization of the system requires taking into consideration not only single-factor effects, but also the cross-factor effects. Therefore, the use of experimental design methodologies (DOE) [12–14] results very suitable to:

- identify the factors affecting a multivariate process;
- fit the empirical models to the experimental data;
- develop statistically significant empirical models [3,15–17].

Specifically, DOE is used in this work to plan the measurements for evaluating the influence of Fenton reagents and contaminant

* Corresponding author. Tel.: +34 93 4137275; fax: +34 93 4137401.
E-mail address: montserrat.perez-moya@upc.edu (M. Pérez-Moya).

concentration on the degradation of organic matter, determined as total organic carbon (TOC). At this point, it should be kept in mind that TOC is a lumped parameter that provides aggregated information instead of the specific concentration data needed for a detailed first principles model.

The execution of the experimental design leads to a set of data including the control or independent variable values (input) and contaminant degradation expressed TOC terms (output). Next step consists of generalizing as much as possible the correlation between input and output values by means of a practical model for predicting the system response.

$$f(x) = a + \sum_i b_i x_i + \sum_i c_i x_i^2 + \sum_{i>j} d_{ij} x_i x_j \quad (5)$$

Assuming a second order polynomial model (from here on quadratic model, Eq. (5)) is of general use for characterizing degradation processes [3,14–18]. This is not the only choice for an empirical model, but it results very helpful in multivariate analysis because learning the influence of the different factors is straightforward from the linear, bilinear and quadratic terms of the equation. Additionally, linear or/and quadratic polynomial models are the implicit options of most of the statistical software available.

The first step in model building is model selection, which is a modeling decision. Next, parameter estimation consists of fitting the model to experimental data by searching the values of the model parameters that best describe these data. The model fitting is defined by an error criterion to be minimized, which is generally the sum of the squares of the differences between the model predictions and the experimental data.

Standard correlation indexes, such as R^2 , allow rating the fitting degree of the model to the data. They are useful for parameter estimation, since the numerical values attained allow comparing the matching of data and models of the same kind, but they may not provide enough information for comparing different kind of models (e.g. involving different number of parameters). However, model selection requires further information and reasoning. On this basis, this work discusses the suitability of different models from the perspective of their structural and inherent features (monotony, symmetry, extreme points) and their consistency with the nature of the process. Alternative models are proposed aimed at superseding the shortcomings detected.

This point may be illustrated by the simple one-dimension case, for which the general quadratic model (Eq. (5)) is reduced to the simple second-order equation (Eq. (6)):

$$f(x) = a + bx + cx^2 \quad (6)$$

$$\frac{dx}{dt} = -kt \rightarrow f(x) = x_0 \exp(-kt) \quad (7)$$

Fitting this equation to simple single-variable first-order kinetics (Eq. (7)) may be acceptable for a series of time-concentration data at early reaction times. However, for wider reaction spans, this model is unsuitable for characterizing the behavior of the system and, even despite acceptable values for the correlation coefficient (R^2), this may lead to the estimation of negative concentrations and inexistent minimum values. This mismatch emerges from the long-term incompatibility of the monotonically decreasing nature of the system and the intrinsic change in the sign of the derivative the quadratic equation imposes.

The quadratic equation fails to accurately model the entire dynamics of systems progressing towards their equilibrium. Therefore, while the quadratic equation may be a fine and reliable approximation for slightly non-linear intervals, it may be

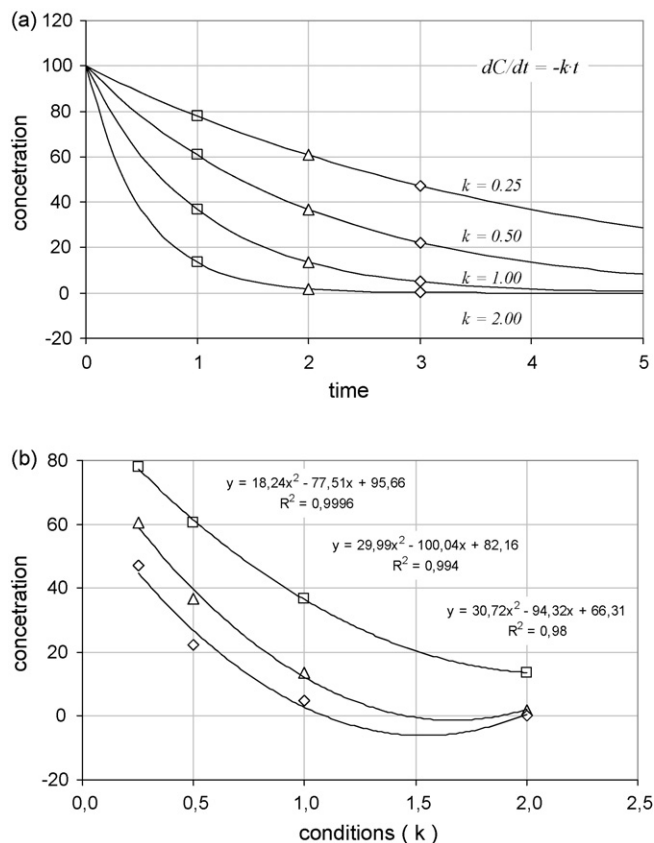


Fig. 1. (a and b) Fitting of a quadratic equation to the data from different conditions.

misleading for highly non-linear intervals. Special caution is required when this model is intended for the determination of optimal conditions (maximums or minimums) because the model is forced to show an extreme point in the interval $(-\infty, \infty)$. Furthermore, the prediction of inconsistent values below zero (or above 100% in case of positive change rates) is strongly related to this behavior.

Certainly, multidimensional systems are difficult to visualize, but the same concepts discussed also apply. For these cases, solving the Hessian matrix of the model allows determining its extreme points. The following example is intended for a final illustration of the analysis introduced and presents the modeling of an indirect correlation for the same first order kinetics case.

Consider perfect experimental data and consider the kinetic rate affected by some extra conditions (other chemicals, temperature, etc.) that may be the object under investigation (Fig. 1). Consider the system evolving as described by Fig. 1a and consider three series of experiments at different times measuring the system response for the different conditions (k).

The data obtained in this series of experiments may be processed as show in Fig. 1b. The slight non-linear dependence on the conditions (k) is well estimated by the quadratic model for the measurements obtained at time 1 (square dots). However, for the data obtained at greater times the fitting of the quadratic model produces inconsistent predictions whose visualization and detection could not be so evident in a multidimensional system. For time 3 (rhombic dots), the parameter fitting may seem quite reliable on the only basis of the correlation coefficient value ($R^2 = 0.98$). Nevertheless, the model prediction regarding Fig. 1b is absolutely inconsistent: an inexistent optimal condition is estimated for $k = 1.5$, for which degradation below zero would be obtained.

The previous single-variable first-order examples are simple cases for which it is clear that no extreme points exist. They are used to illustrate how an inadequate model selection may result in an unreliable prediction capacity of the model, even after the optimization of the parameter values and despite the value of the correlation coefficient. This may also occur in cases of higher complexity. However, the opposite is also possible, and the model may not be able to characterize true extreme points, if any. Thus, the comparative study presented analyses the estimations given by different models, as well as the fitting to the experimental data regarding the number of parameters of each model and the resulting degrees of freedom.

For all the previous examples, as well as the following cases, the parameter fitting is carried out just by means of the minimization of the summation of the square error (SSE). It is worth noting that this is an unconstrained optimization problem allowing the resulting model to produce meaningless estimations (values below zero or above 100%). Thus, given a sufficiently large number of interpolated estimations K , the following constrained problem may be addressed for overcoming this issue:

$$\begin{aligned} \min Z(a, b, c) &= \sum_i (y_i - y_i^*)^2 = \sum_i (y_i - (a + bx_i + cx_i^2))^2 \\ \text{s.t. } y_k^* &= a + bx_k + cx_k^2 \geq 0, \quad \forall k = 1, \dots, K \end{aligned} \quad (8)$$

The solutions obtained are plotted in Fig. 2 and clearly illustrate that, although the model parameters are adjusted in a controlled way that prevents out-of-range estimations, the prediction of an inexistent optimal condition remains, which suggests an inherent incapacity of the type of model to characterize these experimental data. The problems discussed cannot be attributed to parameter fitting, but to inappropriate model selection.

Hence, this work proposes a couple of additional models for a comparative study aimed at assessing their different capacities for fitting to the experimental data from degradation processes. The models proposed are a potential model (Eq. (9), Fig. 3a) and an extended model based on the classical Hoerl equation (Eq. (10), Fig. 3b):

$$f(\mathbf{x}) = a + b \prod_i (x_i + c_i)^{d_i} \quad (9)$$

$$f(\mathbf{x}) = \prod_i (a_i x_i^{b_i} e^{c_i x_i}) = A \prod_i (x_i^{b_i} e^{c_i x_i}) \quad (10)$$

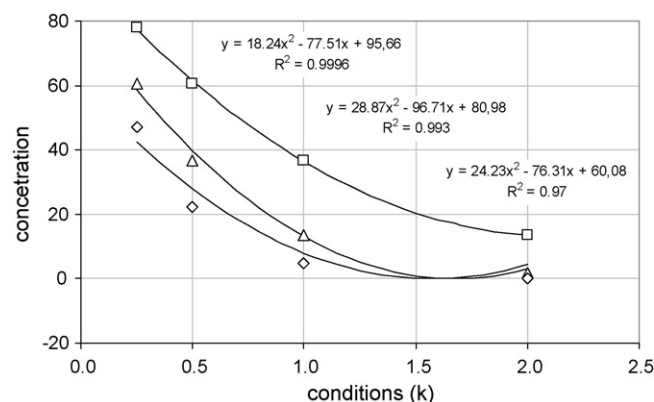


Fig. 2. Fitting of a quadratic equation to the data from different conditions using a constrained least squares minimization.

Both models are empirical models lacking of physical meaning, as the quadratic model. However, they are intended for greater fitting flexibility as well as for allowing the accurate description of strictly monotonic processes. By adjusting the values of their parameters (Fig. 3) both models may be fitted to very different data, and depending on their ratio, they will be not forced to have extreme points (maximum or minimum) while remaining non-linear. The two models proposed allow describing both direct and inverse relationships. In addition, the Hoerl model allows describing non-symmetrical maximums and minimums.

This research addresses the study of the extreme points in the empirical modeling of the degradation of 4-CP as a way to assess the capacity of diverse models to characterize the process. For the simple illustrating examples previously discussed, the determination of extreme points may be achieved either graphically or by solving the single variable equation given by the null derivative condition. For the multivariate case, the study of the Hessian matrix will be required.

Model selection is one of the issues addressed next. The performance of different models characterizing the experimental data will be discussed in depth. However, further than the discussion provided in this paper, an essential issue to be elucidated is what the model is intended for.

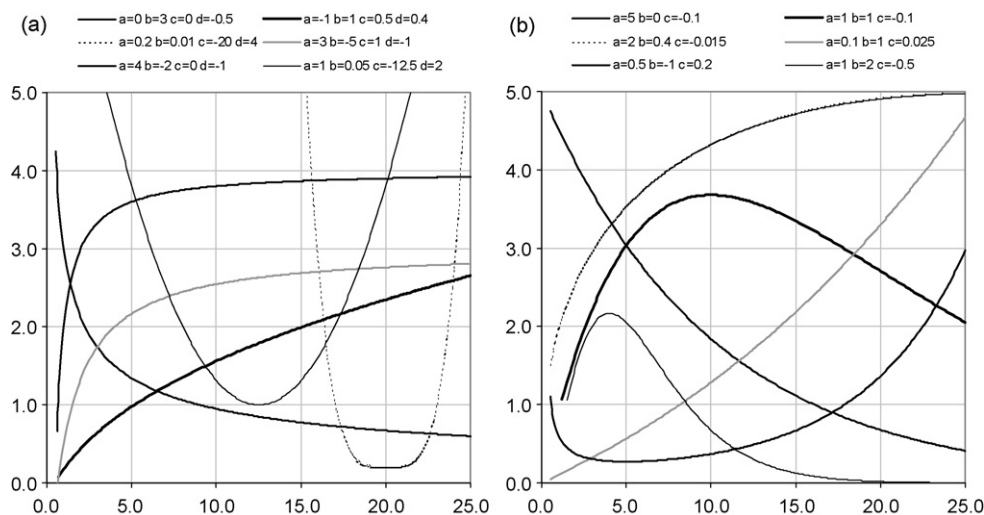


Fig. 3. (a) Potential model, under different coefficients. (b) The classical Hoerl model, under different coefficients.

Table 1

Experimental data of the 4-CP treated by Fenton, Fenton-like and photo-Fenton reactions

| Assay | Codified values | | | Variable levels | | | TOC (ppm) | | | | |
|-------|-----------------|--|--------------|-----------------|--|--------------|---------------------|-----|-----|-----|-----|
| | [Fe(II)] (ppm) | [H ₂ O ₂] (ppm) | [4-CP] (ppm) | [Fe(II)] (ppm) | [H ₂ O ₂] (ppm) | [4-CP] (ppm) | Reaction time (min) | | | | |
| | | | | | | | 0 | 15 | 30 | 45 | 60 |
| 1 | −1 | −1 | −1 | 10 | 200 | 74 | 44 | 32 | 29 | 26 | 24 |
| 2 | +1 | −1 | −1 | 50 | 200 | 74 | 41 | 23 | 17 | 14 | 8 |
| 3 | −1 | +1 | −1 | 10 | 800 | 74 | 42 | 19 | 5 | 0 | 1 |
| 4 | +1 | +1 | −1 | 50 | 800 | 74 | 42 | 18 | 11 | 6 | 4 |
| 5 | −1 | −1 | +1 | 10 | 200 | 222 | 123 | 118 | 122 | 120 | 122 |
| 6 | +1 | −1 | +1 | 50 | 200 | 222 | 123 | 117 | 116 | 116 | 117 |
| 7 | −1 | +1 | +1 | 10 | 800 | 222 | 121 | 91 | 82 | 69 | 54 |
| 8 | +1 | +1 | +1 | 50 | 800 | 222 | 124 | 73 | 54 | 41 | 34 |
| 9 | 0 | 0 | 0 | 30 | 500 | 148 | 88 | 51 | 42 | 37 | 33 |
| 10 | 0 | 0 | 0 | 30 | 500 | 148 | 89 | 47 | 24 | 31 | 11 |
| 11 | 0 | 0 | 0 | 30 | 500 | 148 | 87 | 58 | 52 | 48 | 42 |
| 12 | −1.68 | 0 | 0 | 0 | 500 | 148 | 91 | 96 | 92 | 95 | 96 |
| 13 | 1.68 | 0 | 0 | 64 | 500 | 148 | 86 | 47 | 41 | 36 | 34 |
| 14 | 0 | −1.68 | 0 | 30 | 0 | 148 | 90 | 90 | 92 | 90 | 94 |
| 15 | 0 | 1.68 | 0 | 30 | 1004 | 148 | 79 | 39 | 18 | 10 | 1 |
| 16 | 0 | 0 | −1.68 | 30 | 500 | 24 | 18 | 7 | 3 | 2 | 1 |
| 17 | 0 | 0 | 1.68 | 30 | 500 | 272 | 155 | 127 | 123 | 121 | 119 |

2. Experimental and methods

Analytical grade 4-CP was purchased from Sigma–Aldrich and was diluted to the different specified concentrations as shown in Table 1. Analytical grade hydrogen peroxide and heptahydrated ferrous sulfate were purchased from Panreac and Sigma–Aldrich, respectively, and were used as received. The rest of the chemicals used were, at least, of reagent grade. Solutions were prepared with deionized water obtained from a Millipore Milli-Q system.

Experiments were conducted in a thermostatic cylindrical Pyrex cell. The reaction mixture inside the cell, consisting of 500 mL of 4-CP solution and the precise amount of Fenton reagent, was continuously stirred with a magnetic bar. Temperature was maintained at 40 ± 1 °C along all the reaction time. The initial 4-CP solution pH is 4.5, after adding heptahydrated ferrous sulfate and hydrogen peroxide pH drops and acidic pH, is always kept. pH was on-line measured to ensure its value is kept within the range of 1.5–4 along all the reaction time. Optimal 4-CP degradation is reported [1] to be obtained at pH 2–4, and higher pH values showed to reduce degradation performance.

The experiments were carried out with a sunlight lamp (Ultra-Vitalux[®], Osram, 300 W). The Ultra-Vitalux[®] sunlamp consists of a quartz burner and a tungsten filament which are blended in such a way that the radiation emitted is practically the same as natural sun radiation. The spectral radiation presents wavelengths close to 400 nm (appropriate for photo-Fenton reaction) [7] and up to 550 nm (useful for the Fenton-like reaction) [9]. The distance between the lamp and the reactor's center was 15 cm. Total organic carbon (TOC) of samples was determined with a Shimadzu 5000 TOC analyzer.

DOE was used for planning the experiments and central composite design with star points was applied to determine the influence of Fenton reagent loads (Fe(II), H₂O₂) and the target, 4-CP load. Each variable assumes two levels (low and high), which correspond to the concentration range of every variable specified in Table 1, including three central points for statistical validity and star points at −1.68 to +1.68. The variable levels were set as follows:

- 4-chlorophenol concentration (74–222 mg L^{−1}),
- hydrogen peroxide concentration (200–800 mg L^{−1}) and
- iron concentration (10–50 mg L^{−1}).

Hence, the associated system response is given by the TOC concentration of the system after different reaction times.

3. Results and discussion

3.1. Experimental data

The Fenton, Fenton-like and photo-Fenton reactions were performed on appropriated 4-CP aqueous solutions under different operating condition as summarized in Table 1. In all the cases high and low level is the same for Fenton reagent loads (Fe(II), H₂O₂) and 4-CP load.

The empirical models fitted to these data were evaluated and their significance was analyzed by:

- (1) using the statistical indexes described in Section 3.5 (Eqs. (12–15)). The study also analyzes the model's fitting adjustment (R^2 and Adjusted R^2).
- (2) determining extreme points from the study the corresponding Hessian matrices.

For the sake of clarity the following nomenclature is used from here on:

$$x_1 \rightarrow [4\text{-CP}], x_2 \rightarrow [\text{Fe(II)}], x_3 \rightarrow [\text{H}_2\text{O}_2], f(\mathbf{x}) \rightarrow [\text{TOC}]$$

The experimental data (Table 1) was previously reported in a preliminary work [18], as well as some partial considerations on parameter estimation and model fitting. The initial results demonstrate that additional research was necessary. A further study was conceived in order to assess the different conclusions that may be derived from the different empirical models used to describe the degradation performance of the Fenton and photo-Fenton treatments. Thereby the existence of extreme points was determined and discussed for all the models proposed and their predictive capacity was evaluated and compared.

3.2. Model 1: second order polynomial equation

The usual second order polynomial equation was given by Eq. (5) in the introduction section.

Table 2

Coefficients of the quadratic model in the polynomial expression for different reaction time of the 4-chlorophenol degradation under Fenton reagent enhanced with light radiation

| Reaction time (min) | <i>a</i> | <i>b</i> ₁ | <i>b</i> ₂ | <i>b</i> ₃ | <i>c</i> ₁ | <i>c</i> ₂ | <i>c</i> ₃ | <i>d</i> ₁₂ | <i>d</i> ₁₃ | <i>d</i> ₂₃ |
|---------------------|----------|-----------------------|-----------------------|------------------------|-----------------------|-----------------------|-----------------------|------------------------|------------------------|------------------------|
| 15 | 14.98 | 0.51 | −0.93 | -1.96×10^{-2} | 5.84×10^{-4} | 1.20×10^{-2} | 2.72×10^{-5} | -8.5×10^{-4} | -3×10^{-4} | -2×10^{-4} |
| 30 | 19.84 | 0.46 | −1.21 | -3.53×10^{-2} | 1.08×10^{-3} | 1.89×10^{-2} | 3.48×10^{-5} | -2.43×10^{-3} | -4×10^{-4} | -1.1×10^{-4} |
| 45 | 5.78 | 0.56 | −1.10 | -2.10×10^{-5} | 8.9×10^{-4} | 1.61×10^{-2} | 1×10^{-5} | -2.11×10^{-3} | -5.2×10^{-4} | -1.4×10^{-4} |
| 60 | 20.58 | 0.46 | −1.84 | -1.19×10^{-2} | 1.34×10^{-3} | 2.31×10^{-2} | 3.22×10^{-5} | -8.9×10^{-4} | -7×10^{-4} | -6.8×10^{-5} |

Table 3

Coefficients of the potential model for different reaction time of the 4-chlorophenol degradation under Fenton reagent enhanced with light radiation

| Reaction time (min) | <i>a</i> | <i>b</i> | <i>c</i> ₁ | <i>d</i> ₁ | <i>c</i> ₂ | <i>d</i> ₂ | <i>c</i> ₃ | <i>d</i> ₃ |
|---------------------|----------|-----------------------|-----------------------|-----------------------|-----------------------|------------------------|-----------------------|------------------------|
| 15 | −8.26 | 5.48×10^{-3} | 106.93 | 2.07 | 1.05×10^{-3} | -5.50×10^{-2} | 122.18 | -3.14×10^{-1} |
| 30 | −17.89 | 2.66×10^{-6} | 278.35 | 3.44 | 4.68×10^{-3} | -7.36×10^{-2} | 232.15 | -5.56×10^{-1} |
| 45 | −4.66 | 1.24×10^{-3} | 51.26 | 2.24 | 3.48×10^{-8} | -4.44×10^{-2} | 294.57 | -8.85×10^{-1} |
| 60 | −12.99 | 1.44×10^{-5} | 310.92 | 4.56 | 3.59×10^{-9} | -4.14×10^{-2} | 788.39 | −1.80 |

Table 4

Coefficients of the simplified potential model for different reaction time of the 4-chlorophenol degradation under Fenton reagent enhanced with light radiation

| Reaction time (min) | <i>a</i> | <i>b</i> | <i>c</i> ₂ | <i>c</i> ₃ |
|---------------------|----------|-----------|-----------------------|-----------------------|
| 15 | −13.15 | 180517.01 | 168.85 | 1344.04 |
| 30 | −22.38 | 112503.94 | 136.19 | 875.02 |
| 45 | −25.26 | 97295.28 | 129.26 | 762.25 |
| 60 | −28.57 | 80162.20 | 123.84 | 606.76 |

Fitting the quadratic model to the degradation data for different reaction time allows obtaining the coefficients summarized in Table 2.

3.3. Model 2: potential model

The use of the Potential model, Eq. (9) in Section 1, results in nine degrees of freedom, two more than the previous model.

Degradation experimental data was fit to the Potential model; Table 3 summarizes the coefficient values of the model.

From the studied degradation system, it seems logical to assume that for the contaminant, 4-CP, as direct proportional variable respect the response factor of the system, the parameter *c*₁ will be zero and the parameter *d*₁ will be 1. In the same way, it is possible to assume the reagent variables will behave in inverse relation (*d*₂ = −1 and *d*₃ = −1).

Although the coefficients of the potential model summarized in Table 3, do not confirm this performance the potential model, Eq. (9), was simplified in order to evaluate models with less degrees of freedom.

Assuming the above simplifications, the general polynomial model turns into the following expression:

$$f(x) = a + b \prod_i x_i \prod_{j>i} (x_j + c_j)^{-1} \quad (11)$$

Degradation experimental data was fit to the above-simplified model. Table 4 summarizes the coefficient values of the models.

3.4. Model 3: Hoerl equation

The model based on the Hoerl equation is proposed as a combined product for all the variables contributing to the system response, Eq. (10) in the introduction section Table 5 summarizes the coefficient values of the model.

3.5. Discussion of the modeling assessment: comparing the empirical model quality

The least squares criterion was used for fitting the models and adjusting the values of the corresponding parameters. Hence, the analysis of variance (ANOVA) was used to evaluate the significance of the multiple-regression performed. For the quantitative discussion, the fitting performance of each model is measured with the following indexes.

3.5.1. Residual values

The total sum of square differences between an observed value (*y*) and its corresponding fitted value (*ŷ*) represents a measure of variation or deviation from the mean (*ȳ*). This is the sum square error (SSE)

$$SSE = \sum_{i=1}^n (y_i - \hat{y}_i)^2 \quad (12)$$

The least squares criterion aims at minimizing the SSE value so as to obtain the optimal model's parameters.

3.5.2. Coefficient of multiple determination (*R*²)

With the aim to introduce the coefficient of multiple determination it is necessary to establish the residual sum of squares (the total sum of squares (TSS) = regression sum of squares (SSR) + residual sum of squares (SSE), Eq. (12)), which is the variation attributed to the error.

$$TSS = \sum_{i=1}^n (y_i - \bar{y})^2 = \sum_{i=1}^n (\hat{y}_i - \bar{y})^2 + \sum_{i=1}^n (y_i - \hat{y}_i)^2 \quad (13)$$

Table 5

Coefficients of the Hoerl function for different reaction times of the 4-chlorophenol degradation under Fenton reagent enhanced with light radiation

| Reaction time (min) | <i>a</i> | <i>b</i> ₁ | <i>c</i> ₁ | <i>b</i> ₂ | <i>c</i> ₂ | <i>b</i> ₃ | <i>c</i> ₃ |
|---------------------|-----------------------|-----------------------|-----------------------|------------------------|------------------------|------------------------|------------------------|
| 15 | 2.26×10^{-1} | 1.14 | 1.54×10^{-3} | -1.04×10^{-2} | -2.21×10^{-3} | -4.14×10^{-3} | -6.14×10^{-4} |
| 30 | 6.56×10^{-2} | 1.37 | 2.05×10^{-3} | -1.40×10^{-2} | -2.91×10^{-3} | -5.17×10^{-3} | -1.02×10^{-3} |
| 45 | 6.98×10^{-2} | 1.33 | 2.90×10^{-3} | -1.77×10^{-2} | -2.13×10^{-3} | -4.42×10^{-3} | -1.30×10^{-3} |
| 60 | 1.57×10^{-1} | 1.07 | 6.12×10^{-3} | -2.34×10^{-2} | -1.12×10^{-3} | -5.93×10^{-3} | -1.72×10^{-3} |

Table 6

Sum of squared error (SEE) of the models applied to the experimental data at the different reaction times

| Model | Function | Degrees of freedom | Reaction time (min) | | | |
|-------|----------------------------|--------------------|---------------------|--------|--------|--------|
| | | | 15 | 30 | 45 | 60 |
| 1 | Quadratic model | 7 | 936.0 | 1578.0 | 1667.8 | 2358.5 |
| 2 | Potential model | 9 | 187.9 | 800.8 | 794.3 | 1020.0 |
| 2s | Simplified potential model | 13 | 1285.0 | 2479.3 | 2862.2 | 4440.6 |
| 3 | Hoerl equation | 10 | 233.2 | 922.4 | 665.6 | 969.1 |

The coefficient of multiple determination measures the amount of variation of the response variable that is explained by the predictor variable(s). In general, the closer R^2 approaches 1.0, the better the model fits the data.

$$R^2 = 1 - \frac{\sum_{i=1}^n (y_i - \hat{y}_i)^2}{\sum_{i=1}^n (y_i - \bar{y})^2} \quad (14)$$

3.5.3. Adjusted R^2 (Adj- R^2)

R^2 , the coefficient of multiple determination, will always increase when a new parameter is added to the model. A model with more terms may appear to have a better fit simply because it has more parameters to be adjusted (or less degrees of freedom). In order to compare the quality of the different proposed empirical models and balance their different degrees of freedom it is important to use an index as the Adjusted R^2 .

$$\text{Adjusted } R^2 = 1 - \frac{\sum_{i=1}^n (y_i - \hat{y}_i)^2 / n - p}{\sum_{i=1}^n (y_i - \bar{y})^2 / n - 1} \quad (15)$$

where n is the number of experiments performed and p is the fit coefficient number.

The Adj- R^2 is a useful index for comparing the explanatory power of models with different numbers of predictors. The Adj- R^2 will increase only if the addition of a new parameter improves the model more than would be expected by chance. Otherwise, its value decreases. The closer (Adj- R^2) approaches 1, the better the model fits the data. Tables 6 and 7 show the values for these indexes for the different models.

Results summarized in Tables 6 and 7 demonstrate that the models proposed based on the potential equation (Model 2) and the Hoerl equation (Model 3) produce a much better fitting to the experimental data than the usual quadratic model (Model 1). This is not only assured under an absolute criterion such as the residual values (Table 6) as well as a relative measure such as the adjusted coefficient of multiple determination (Adj- R^2 in Table 7). Furthermore, Model 2 and/or 3 require fewer parameters than Model 1, which means that Model 2 and/or 3 may be used with less experimental data or that, given the same data, fitting Model 2 and/

or 3 are not as tight as fitting Model 1. Certainly, these considerations favoring Models 2 and 3 upon Model 1, both empirical, are merely statistical, but further reasoning is not possible unless first principles models are introduced.

The analysis of the residual values reveals that the potential model (Model 2) fits better the experimental data than the simplified potential model (Model 2s). Additionally, although the general model (2) requires four parameters more than the simplified model (2s), the Adj- R^2 index shows that these parameters improve the model fitting more than it would be expected just by chance; thus, they may not be neglected. Given these results, further study of the simplified model was considered unnecessary.

For clarifying the assessment of the model fitting, measured and predicted values are compared in Fig. 4 (45 min). The numerical information in Tables 6 and 7 quantifies the global agreement between the data and the model and denotes good model fitting. However, deeper and particular analysis is required for assessing the prediction capacity of the models. For instance, the prediction of negative TOC values (Fig. 4, assay 16) should be accounted as a failure of the quadratic model. Models 2 and 3 are not estimating negative values despite these meaningless values are mathematically allowed in the optimization procedure for fitting all model parameters. Further investigation may be undertaken for constraining the model fitting (whichever model considered) to positive values.

Once model fitting and parameter estimation is complete, the resulting models are analyzed regarding the estimations each one is producing. The study of the extrema (maxima and/or minima) predicted by the different models is detailed in the following Tables 8 and 9 [19]. Table 8 shows the stationary points estimated by the first derivative test. For all reaction times in the second column, the coordinates of the candidate points are given in the third, fourth and fifth column.

For the polynomial and the Hoerl models, these points not only lay out of the interpolation domain, but they are physically meaningless, which prove the inexistence of stationary points according to these models. Conversely, the quadratic model shows four candidate points: two beyond the boundaries of the

Table 7 R^2 and Adj- R^2 for the models proposed

| Model | Function | Degrees of freedom | Reaction time (min) | | | |
|----------------|----------------------------|--------------------|---------------------|-------|-------|-------|
| | | | 15 | 30 | 45 | 60 |
| R^2 | | | | | | |
| 1 | Quadratic model | 7 | 0.960 | 0.944 | 0.943 | 0.927 |
| 2 | Potential model | 9 | 0.992 | 0.972 | 0.973 | 0.969 |
| 2s | Simplified potential model | 13 | 0.945 | 0.912 | 0.902 | 0.863 |
| 3 | Hoerl equation | 10 | 0.990 | 0.967 | 0.977 | 0.970 |
| Adjusted R^2 | | | | | | |
| 1 | Quadratic model | 7 | 0.909 | 0.872 | 0.870 | 0.834 |
| 2 | Potential model | 9 | 0.986 | 0.950 | 0.952 | 0.944 |
| 2s | Simplified Potential model | 13 | 0.933 | 0.892 | 0.880 | 0.831 |
| 3 | Hoerl equation | 10 | 0.984 | 0.948 | 0.964 | 0.952 |

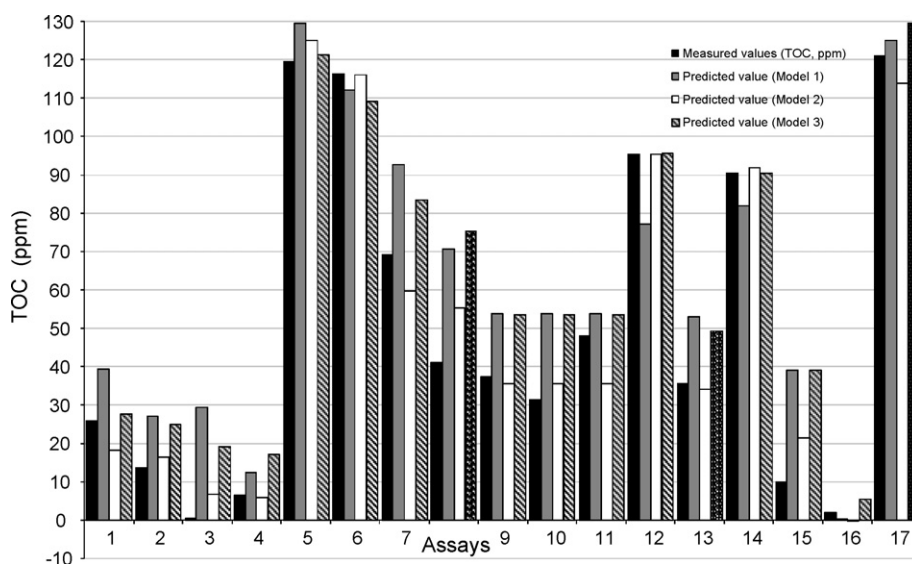


Fig. 4. Measured and predicted system response (45 min) compared for each assay.

Table 8

Second derivative test for the models proposed

| Model | Time (min) | [4-CP] (ppm) | [Fe(II)] (ppm) | [H ₂ O ₂] (ppm) | Interpolation domain | $ Hf(x_1, x_2, x_3) $ |
|------------|------------|--------------|----------------------|--|----------------------|------------------------|
| Quadratic | 15 | 616.23 | 93.55 | 3901.02 | OUT | – |
| | 30 | 124.57 | 45.87 | 1496.08 | OUT | – |
| | 45 | 27.57 | 40.51 | 1001.37 | IN | -7.98×10^{-9} |
| | 60 | 54.15 | 42.02 | 817.83 | IN | -1.49×10^{-8} |
| Polynomial | 15 | –106.93 | $(-\infty, +\infty)$ | $(-\infty, +\infty)$ | OUT | – |
| | 30 | –278.35 | $(-\infty, +\infty)$ | $(-\infty, +\infty)$ | OUT | – |
| | 45 | –51.27 | $(-\infty, +\infty)$ | $(-\infty, +\infty)$ | OUT | – |
| | 60 | –310.92 | $(-\infty, +\infty)$ | $(-\infty, +\infty)$ | OUT | – |
| Hoerl | 15 | –737.06 | –4.71 | –6.79 | OUT | – |
| | 30 | –668.11 | –4.83 | –5.07 | OUT | – |
| | 45 | –459.32 | –8.29 | –3.40 | OUT | – |
| | 60 | –174.07 | –20.88 | –3.31 | OUT | – |

experimental design, and two within the interpolation domain. Bearing in mind the considerations and the examples discussed in the introduction it should not be strange that the quadratic model may produce maximum or minimum estimations for those time values closer to the equilibrium.

Since the extrapolated estimations are unreliable for an empirical model, the following considerations refer only to the stationary points estimated by the quadratic model at $t = 45'$ and $t = 60'$. The second derivative test allows elucidating the nature of these stationary points. The negative values of the determinant of the corresponding Hessian matrix (last column in Table 8) indicate that they are not optimal values. However, there is evidence that, regarding a particular direction, extreme values may be predicted at these points. This situation is studied in Table 9.

Table 9

Second derivative test for the quadratic model at 45 and 60 min reaction time

| Time (min) | Fixed variable x_i (ppm) | $ Hf(x_j, x_k) $ | $\partial^2 f / \partial x_j^2$ | Max/Min | Interpolation domain |
|------------|--|------------------|---------------------------------|-------------|----------------------|
| 45 | [4-CP] = 27.57 | + | + | Minimum | IN |
| | [Fe(II)] = 40.51 | – | – | Non extreme | IN |
| | [H ₂ O ₂] = 1001.37 | + | + | Minimum | IN |
| 60 | [4-CP] = 54.15 | + | + | Minimum | IN |
| | [Fe(II)] = 42.02 | – | – | Non extreme | IN |
| | [H ₂ O ₂] = 817.83 | + | + | Minimum | IN |

Three particular cases are obtained when each variable is fixed.

Table 9 shows the sign of the minor Hessian determinant for the conditions given by the fixed value of one coordinate. The positive signs indicate an extreme value in the direction of the rest of the coordinates. For these values the sign of the first diagonal element of the Hessian matrix shows that all the extrema determined by the quadratic model are minima.

3.6. Discussion of the multifactor system: photo-assisted Fenton degradation

The statistical study demonstrates that models are consistent for the whole reaction span. However, the second derivative test proves that only for the quadratic model the existence of minimum values is predicted. These discrepant model estima-

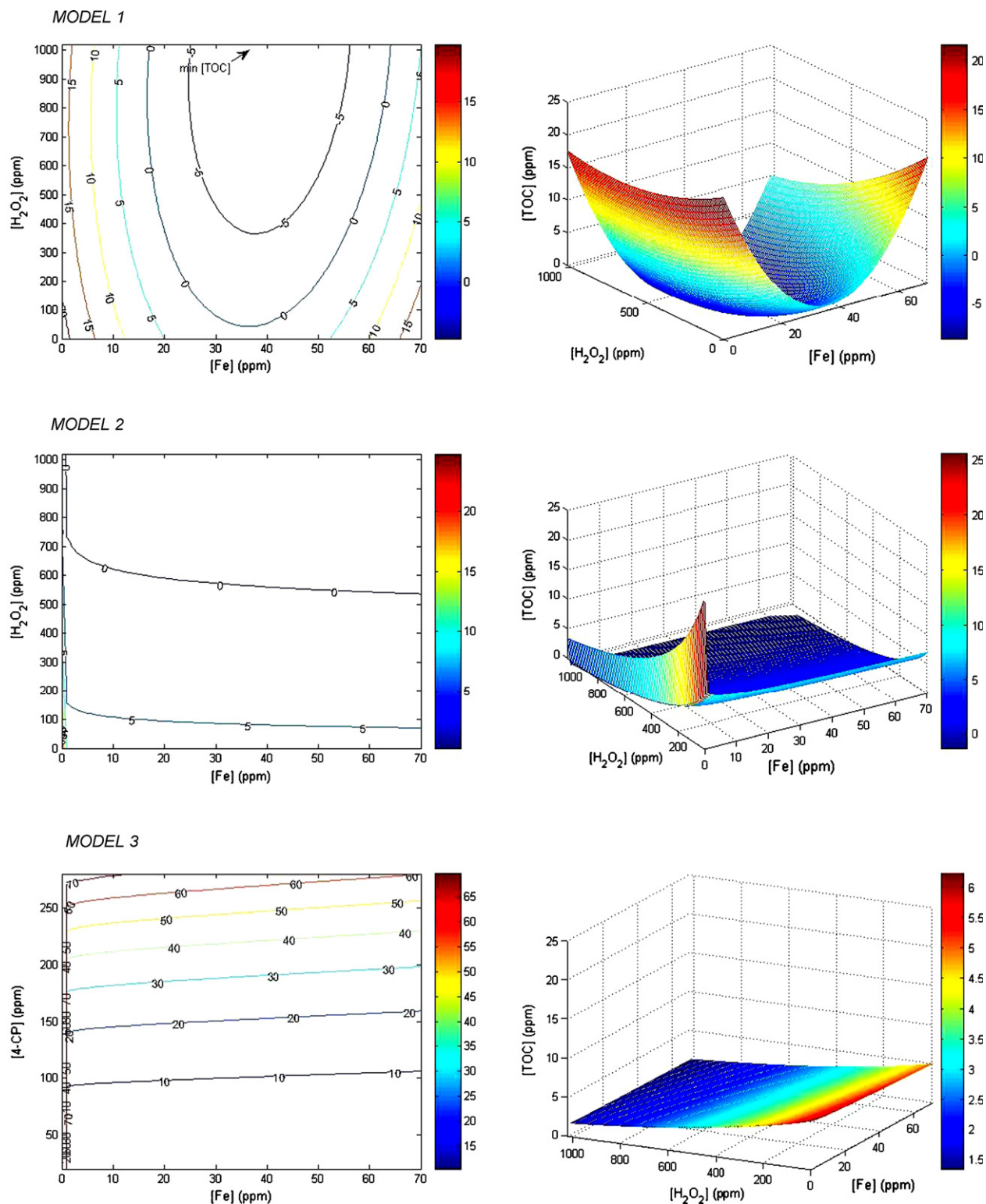


Fig. 5. Two and three-dimensional response surface representation for the TOC remaining after 45 min of reaction. 4-CP load is fixed at 27.57 ppm (minimum value obtained in the extreme study). In three-dimensional representation Fe(II) and H_2O_2 load are represented in the abscissa while the TOC remaining is shown in the ordinate.

tions, already observed in Fig. 4, are clearly envisaged through the response surface plots for the minimum values found in quadratic model.

Response surfaces for the three models studied are given in Figs. 5 and 6 for reaction times 45 and 60 min. In Fig. 5, 4-CP load is

fixed at 27.57 ppm (the minimum value obtained for this variable from the first derivative test). In Fig. 6, H_2O_2 load is fixed at 1001 ppm (the minimum value obtained for this variable from the first derivative test). Clearly, the trends revealed by each model are totally different. Despite no physicochemical constraints were

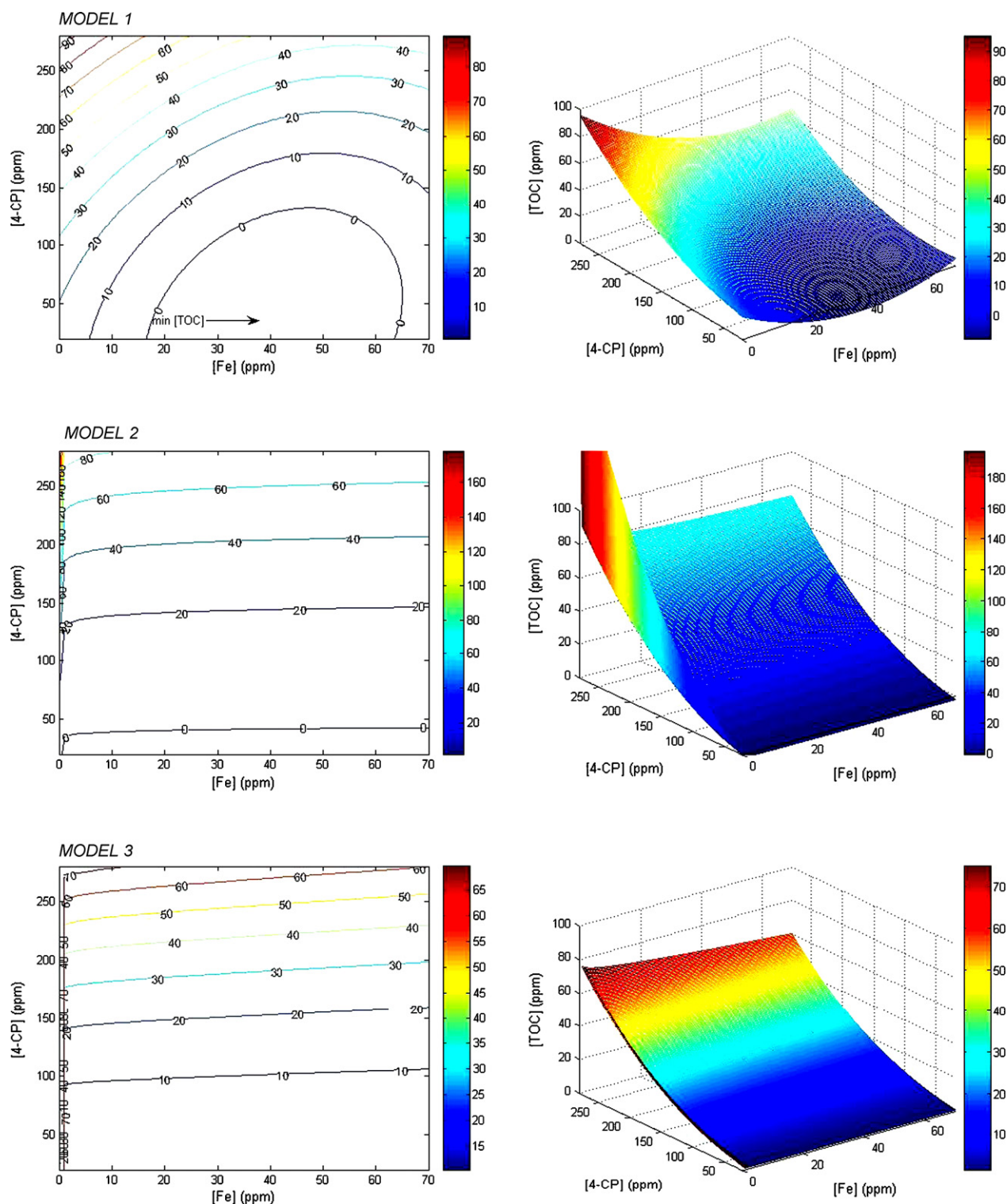


Fig. 6. Two-dimensional and three-dimensional representation of the response surface for the TOC remaining after 45 min of reaction. H_2O_2 load is fixed at 1001 ppm (minimum value obtained in the extreme study). In three-dimensional representation, 4-CP and Fe(II) load are represented in the abscissa while the TOC remaining is shown in the ordinate.

considered for fitting the models to the data, and despite parameters were adjusted just in order to minimize a pure mathematical criterion such as the quadratic error, each model is leading to unexpected different conclusions.

Apart from the meaningless negative values predicted by the quadratic model, (Fig. 7) the model is also forcing stationary

points that are quite questionable. In the same way the potential model is forcing an asymptotic behavior that may also be uncertain.

However, the study of several Fenton reagent loads allows choosing a proper reagent ratio within practical and qualitative limits. Appropriate reagent load leads to TOC reduction up to close

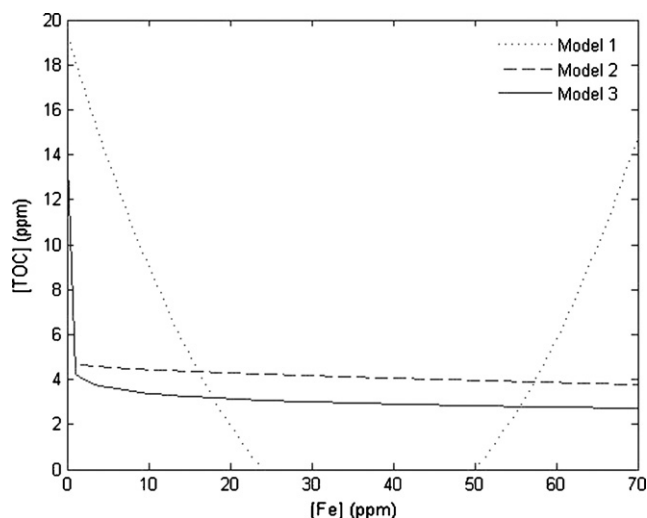


Fig. 7. TOC remaining after 45 min of reaction. 4-CP load is fixed at 27.57 ppm (minimum value obtained in the extreme study) and H_2O_2 load is fixed at 200 ppm (the low value from the experimental design). Fe(II) load are represented in the abscissa while the TOC remaining is shown in the ordinate.

100% for the lowest 4-CP concentration (74 mg L^{-1}) and around 80% for highest 4-CP concentration (222 mg L^{-1}). Regardless the contrasting estimations obtained by the different models (Figs. 5 and 6) for the minima value of the system ($[\text{4-CP}] = 27.57 \text{ ppm}$, $[\text{H}_2\text{O}_2] = 1001 \text{ ppm}$, $[\text{Fe(II)}] = 40.5 \text{ ppm}$) at 45 min reaction time, the TOC prediction of quadratic model is -8.92 ppm , and for potential model -1.44 ppm . Both are negative meaningless values that should be considered as 0. Thus, the process permits TOC total reduction. For the same conditions the Hoerl model estimates a residual TOC value of 1.42 ppm, which maybe also regarded as an estimation of total TOC remediation in practical terms. Similar results are obtained after 60 min reaction but the minimum value of the system is placed at ($[\text{4-CP}] = 54.1 \text{ ppm}$, $[\text{H}_2\text{O}_2] = 817.8 \text{ ppm}$, $[\text{Fe(II)}] = 42.0 \text{ ppm}$). Iron load is quite similar in both reaction times.

Fig. 7 allows further comparative analysis regarding the prediction capacity of each model by plotting the system response to iron load at given time, contaminant and peroxide conditions ($[\text{4-CP}] = 27.57 \text{ ppm}$, $[\text{H}_2\text{O}_2] = 200 \text{ ppm}$ and $t = 45'$). Fig. 7 demonstrates that while the potential and Hoerl models are producing quite similar estimations, the quadratic model is leading to surprisingly disparate predictions.

According to the potential and Hoerl models, the degradation process (including Fenton, Fenton-like and photo-Fenton reactions) is moderately and monotonically depending on the iron load and the degradation rate is always increasing along with the iron concentration.

Conversely, according to the quadratic model, increasing iron concentration increases the degradation rate only up to a certain iron concentration, for which this trend is reversed. Beyond this maximum degradation rate, the quadratic model predicts that increasing iron load will result in more and more degradation inefficiency.

4. Conclusions

The Fenton photo-assisted treatment process has been studied for the degradation of 4-chlorophenol (4-CP). The experimental data has been obtained for a series of conditions arranged under a design of experiments scheme and practical operational conclusions have been obtained.

For the 4-CP concentration range studied appropriate reagent loads have been obtained producing TOC reduction rates from 80% to almost 100% when the treatment was allowed to proceed during 45 min. For 60 min reaction time the system clearly evolved to total 4-CP remediation. Iron loads around 40 ppm lead to adequate TOC degradation for the complete studied span.

The mathematical modeling of this degradation process has been undertaken by fitting a set of empirical functions to the experimental data. Comparing the models has revealed how the widely used quadratic model may produce low residual values at the expense of a significant number of parameters. Conversely, a model may be proposed requiring fewer parameters, as well as producing lower residuals. This is achieved by a model based on the classical Hoerl function. Thus, the conventional quadratic model may be useful and intuitive regarding the detection of variable cross-over. However, it may force the prediction of maxima and/or minima that cannot be completely guaranteed and that are not estimated by other models fitted to the same data. This is particularly evident for situations close to the equilibrium.

Additionally, high values for the standard correlation values have demonstrated to provide incomplete insight on the real correspondence between this trend and the data. The analysis of the graphical information has revealed very useful in discerning the lack of correspondence between the predictions given by the three different models studied. Furthermore, the quantitative difference between the response surfaces given these models may reach 25% in certain cases.

Although the modeling performed is purely empirical and it is not intended for representing the actual driving force (or principle) of the process, it should be expected to result in the estimation of reliable degradation values. This research demonstrates that this is not the case and further research is required for guaranteeing the prediction of the conditions of the most favorable TOC reduction, since it could significantly depend on the model selected. Certainly, for addressing this modeling issue an important aspect is to clearly define what the model is intended for.

Acknowledgement

We would like to thank the financial support received from Spanish "Ministerio de Educación y Ciencia" through Project DPI2006-0567.

References

- [1] M. Pera-Titus, V. García-Molina, M.A. Baños, J. Jiménez, S. Esplugas, *Appl. Catal. B: Environ.* 47 (2004) 219–256.
- [2] M. Rodríguez, S. Malato, C. Pulgarin, S. Contreras, D. Curcó, J. Jiménez, S. Esplugas, *Sol. Energy* 79 (2005) 360–368.
- [3] A.G. Trovó, W.C. Paterlini, R.F.P. Nogueira, J. Hazard. Mater. B137 (2006) 1577–1582.
- [4] P. Raja, A. Bozzi, W.F. Jardim, G. Mascolo, R. Renganathan, J. Kiwi, *Appl. Catal. B: Environ.* 59 (2005) 249–257.
- [5] H.J.H. Fenton, *J. Chem. Soc.* 65 (1894) 899–910.
- [6] J.J. Pignatello, *Environ. Sci. Technol.* 26 (1992) 944–951.
- [7] A. Safarzadeh-Amiri, J.R. Bolton, S.R. Cater, J. Adv. Oxid. Technol. 1 (1996) 18–26.
- [8] S.H. Bossmann, E. Oliveros, S. Göb, S. Siegwart, E.P. Dahlen, L.M. Payawan, M. Straub, M. Wörner, A.M. Braun, J. Phys. Chem. 102 (1998) 5542–5550.
- [9] J.J. Pignatello, D. Liu, P. Huston, *Environ. Sci. Technol.* 33 (1999) 1832–1839.
- [10] G. Sagawe, A. Lehnard, M. Lubber, D. Bahnemann, *Helv. Chim. Acta* 84 (2001) 3742–3759.
- [11] H. Kušić, N. Koprivanac, A. Lončarić, I. Selanec, J. Hazard. Mater. B136 (2006) 632–644.
- [12] D.C. Montgomery, *Design and Analysis of Experiments*, 5th ed., John Wiley & Sons, New York, 2001.
- [13] D. Cuthbert, *Fitting Equations to Data; Computer Analysis of Multifactor Data*, 2nd ed., John Wiley & Sons, New York, 1980.

- [14] G.E.P. Box, W.G. Hunter, J.S. Hunter, *Statistics for Experimenters: An Introduction to Design, Data Analysis and Model Building*, Wiley, New York, 1978.
- [15] M. Rios-Enriquez, N. Shahin, C. Durán-de-Bazúal, J. Lang, E. Oliveros, S.H. Bossmann, A. Braun, *Sol. Energy* 77 (2004) 491–501.
- [16] E. Oliveros, O. Legrini, M. Hohl, T. Müller, A.M. Braun, *Chem. Eng. Process.* 36 (1997) 397–405.
- [17] J.H. Ramirez, C.A. Costa, L.M. Madeira, *Catal. Today* 107 (2005) 68–76.
- [18] M. Pérez-Moya, M. Graells, P. Buenestado, E. Gutiérrez, J. Galindo, H.D. Mansilla, *Modelling approach to Fenton and photo-Fenton treatments*, The Proceedings of the 13th International Conference on Advanced Oxidation Technologies for Treatment of Water, Air and Soil. Niagara Falls, New York, USA, 2007.
- [19] S.C. Chapra, *Applied Numerical Methods with Matlab for Engineers and Scientists*, 2nd ed., Mc Graw Hill, 2007.